

Application of precise $^{142}\text{Nd}/^{144}\text{Nd}$ analysis of small samples to inclusions in diamonds (Finsch, South Africa) and Hadean Zircons (Jack Hills, Western Australia)

G. Caro ^{a,*}, V.C. Bennett ^b, B. Bourdon ^c, T.M. Harrison ^{b,d}, A. von Quadt ^c,
S.J. Mojzsis ^e, J.W. Harris ^f

^a *Laboratoire Géochimie-Cosmochimie, Institut de Physique du Globe de Paris, Université Paris 7 Denis Diderot, 4 place Jussieu, 75252 Paris cedex 05, France*

^b *Research School of Earth Sciences, Australian National University, Canberra, A.C.T. 0200, Australia*

^c *Institute of Isotope Geochemistry and Mineral Resources, ETH Zurich, Clausiusstrasse 25, 8092, CH-8092 Zürich, Switzerland*

^d *Department of Earth and Space Sciences and IGPP, University of California, Los Angeles, Los Angeles, California 90095, USA*

^e *Department of Geological Sciences, University of Colorado, Boulder, CO 80303-0399, USA*

^f *Department of Geographical and Earth Sciences, University of Glasgow, Glasgow, G12 8QQ, UK*

Received 9 April 2007; received in revised form 22 October 2007; accepted 27 October 2007

Editor: S.L. Goldstein

Abstract

^{146}Sm – ^{142}Nd and ^{147}Sm – ^{143}Nd systematics were investigated in garnet inclusions in diamonds from Finsch (S. Africa) and Hadean zircons from Jack Hills (W. Australia) to assess the potential of these systems as recorders of early Earth evolution. The study of Finsch inclusions was conducted on a composite sample of 50 peridotitic pyropes with a Nd model age of 3.3 Ga. Analysis of the Jack Hills zircons was performed on 790 grains with ion microprobe $^{207}\text{Pb}/^{206}\text{Pb}$ spot ages from 3.95 to 4.19 Ga. Finsch pyropes yield $100 \times \epsilon^{142}\text{Nd} = -6 \pm 12$ ppm, $\epsilon^{143}\text{Nd} = -32.5$, and $^{147}\text{Sm}/^{144}\text{Nd} = 0.1150$. These results do not confirm previous claims for a 30 ppm ^{142}Nd excess in South African cratonic mantle. The lack of a ^{142}Nd anomaly in these inclusions suggests that isotopic heterogeneities created by early mantle differentiation were remixed at a very fine scale prior to isolation of the South African lithosphere. Alternatively, this result may indicate that only a fraction of the mantle experienced depletion during the first 400 Myr of its history. Analysis of the Jack Hills zircon composite yielded $100 \times \epsilon^{142}\text{Nd} = 8 \pm 10$ ppm, $\epsilon^{143}\text{Nd} = 45 \pm 1$, and $^{147}\text{Sm}/^{144}\text{Nd} = 0.5891$. Back-calculation of this present-day $\epsilon^{143}\text{Nd}$ yields an unrealistic estimate for the initial $\epsilon^{143}\text{Nd}$ of -160 ϵ -units, clearly indicating post-crystallization disturbance of the ^{147}Sm – ^{143}Nd system. Examination of $^{146,147}\text{Sm}$ – $^{142,143}\text{Nd}$ data reveals that the Nd budget of the Jack Hills sample is dominated by non-radiogenic Nd, possibly contained in recrystallized zircon rims or secondary subsurface minerals. This secondary material is characterized by highly discordant U–Pb ages.

* Corresponding author. Present address. Division of Geological and Planetary Sciences, California Institute of Technology, 1200 E. California Blvd, MC 170-25, Pasadena CA 91125, USA.

E-mail address: caro@gps.caltech.edu (G. Caro).

Although the mass fraction of altered zircon is unlikely to exceed 5–10% of total sample, its high LREE content precludes a reliable evaluation of ^{146}Sm – ^{142}Nd systematics in Jack Hills zircons.

© 2007 Elsevier B.V. All rights reserved.

Keywords: Isotope; Differentiation; Hadean crust; Jack Hills; Finsch; ^{142}Nd

1. Introduction

^{146}Sm α -decays to ^{142}Nd with a half-life of 103 Ma. Owing to the low initial abundance of ^{146}Sm in the solar system, the ^{146}Sm – ^{142}Nd chronometer is effectively extinct by ~ 4.2 Ga, and therefore represents a tracer sensitive to the earliest stages of planetary differentiation. While the first attempts to apply this system to terrestrial evolution yielded controversial results (Goldstein and Galer, 1992; Harper and Jacobsen, 1992; McCulloch and Bennett, 1993; Sharma et al., 1996), technical improvements in thermal-ionization mass spectrometry have refined the search for ^{142}Nd anomalies in terrestrial samples (e.g., Caro et al., 2003, 2006; Boyet and Carlson, 2006). The purpose of this study was to use these new analytical techniques to measure ^{142}Nd at high precision in key but rare samples of low Nd content — pyrope inclusions in 3.3 Gyr old diamonds (Finsch mine, South Africa,) and in ≥ 3.9 Gyr old zircons from the Jack Hills (Yilgarn craton, Western Australia). Finsch inclusions and Jack Hills zircons are amongst the oldest preserved samples of the terrestrial mantle and crust (Froude et al., 1983; Richardson et al., 1984; Wilde et al., 2001). The ^{142}Nd record of Jack Hills zircons could provide information about the age and chemical composition of the protocrust, while inclusions in diamonds offer a unique opportunity to investigate small scale ^{142}Nd heterogeneities in Archean mantle.

None of these samples has been investigated at high precision for ^{146}Sm – ^{142}Nd . However, a ~ 30 ppm ^{142}Nd anomaly was recently reported in a lherzolitic nodule from Kimberley (South Africa) (Jagoutz and Dreibus, 2003), which was interpreted as reflecting very early (>4.4 Ga) isolation of South African lithospheric mantle. Oxygen isotope and trace element compositions of pre-4.0 Ga zircons have been used to argue for the role of hydrous peraluminous melts in the generation of granitic crust in the Hadean (Mojzsis et al., 2001; Trail et al., 2007a). The hafnium isotopic composition of Hadean zircons was also shown to indicate early (~ 4.5 Ga) extraction of a terrestrial crust (Harrison et al., 2005). The formation of these lithospheric reservoirs could be related to a process of crystallization and differentiation in a deep magma ocean (Herzberg et al., 1988; Caro et al., 2005).

Both zircons and inclusions in diamonds are *a priori* expected to provide a well-preserved ^{142}Nd record. Zircons, in their unaltered crystalline form, are characterized by very low REE diffusivities (Cherniak et al., 1997) which makes their Sm–Nd isotopic characteristics highly resistant to resetting under crustal conditions. Pyrope inclusions are also expected to have remained effectively isolated from chemical and isotopic exchange with surrounding mantle as their encapsulation in diamonds effectively inhibits such exchanges (Richardson et al., 1984). In this paper, we describe analytical techniques allowing the determination of ± 10 ppm Nd isotope ratios in small samples (10–20 ng Nd) and report the first ^{142}Nd measurements in garnet and zircon composites.

2. Analytical techniques

2.1. Sample selection and chemical separation

2.1.1. Pyrope inclusions

The study of Finsch inclusions was conducted on 50 lilac, Cr-pyrope crystals (~ 3.9 mg) recovered from monocrystalline diamonds using the techniques previously described in Richardson et al. (1984). Inclusions were first gently leached in 3 N HNO_3 and dissolved in 50% HF at 140 °C over 24 hours. 20% of the dissolved solution was aliquoted and spiked using a mixed ^{149}Sm – ^{150}Nd tracer for determination of $^{147}\text{Sm}/^{144}\text{Nd}$. Both fractions were then passed through a 200 μL cationic column. Mg and Al were eluted in 1.5 mL of 2 N HCl and REE were subsequently recovered in 1 mL 4 N HCl. REE fractions for spiked and unspiked aliquots were then introduced onto HDEHP columns (200 μl) and Nd and Sm were separated following the procedures described in the next section. Chemistry yield was 90–95% for both aliquots. Sm and Nd blanks were 10 and 30 pg respectively for the main fraction and 1–3 pg for the spiked aliquot. No blank correction was necessary.

2.1.2. Jack Hills zircons

Application of ^{146}Sm – ^{142}Nd chronometry typically requires precisions of ca. 5–10 ppm on the $^{142}\text{Nd}/^{144}\text{Nd}$ ratio (e.g., Caro et al., 2003). Because Nd ionization yields in thermal ionization mass spectrometry is limited to a few

percent, ^{146}Sm – ^{142}Nd chronometry of Jack Hills zircons requires a minimum of 10–20 ng Nd. Because zircons typically contain only 1–10 ppm Nd (Hoskin and Schaltegger, 2003), this can only be achieved by analyzing composite samples of the small (~1–10 μg) Jack Hills zircons. For the purpose of this study, 790 zircons were therefore selected from about 30,000 grains from the original Jack Hills metaquartzite sample JH992 following $^{207}\text{Pb}/^{206}\text{Pb}$ age analysis (Mojzsis et al., 2001). The grains were initially embedded in epoxy mounts and polished to reveal an internal section. The mounts, containing several hundred zircons each, were analyzed initially in reconnaissance mode to detect all grains with high $^{207}\text{Pb}/^{206}\text{Pb} > 0.42$ (~4 Ga). Those grains were then reanalyzed by standard SHRIMP methods to determine their ages (Ireland et al., in press). Grains with >90% concordant $^{207}\text{Pb}/^{206}\text{Pb}$ ages from 3.95 to 4.19 Ga were then handpicked from the epoxy mounts for Nd isotope analysis.

The composite sample was first leached in 3 N HNO_3 and acetone to remove traces of epoxy and dust from the grains. Zircons were then introduced in a Savillex Teflon vial filled with 0.75 mL 50% HF. The vial was placed in a metal jacketed acid digestion bomb and heated at 200 °C for 7 days. Following dissolution, the sample was dried down on a hotplate and the residue subsequently dissolved in 1 mL 0.1 N H_2SO_4 . After complete dissolution, two 100 μL fractions were aliquoted for determination of Sm and Nd concentrations, and a 10 μL fraction was aliquoted for Pb and Hf isotope analyses. The remaining fraction was dedicated to Nd isotope analysis. Chemical and analytical methods for $^{146,147}\text{Sm}/^{142,143}\text{Nd}$ systematics are described below.

The Sm–Nd aliquot was spiked with a mixed ^{149}Sm – ^{150}Nd tracer calibrated beforehand against NIST SRM 3147a (Sm) and 3135a (Nd). 900 μL of 0.1 N H_2SO_4 was then added to the spiked aliquot to make a total volume of 1 mL 0.1 N H_2SO_4 . The Sm–Nd aliquot and the main fraction were then slowly evaporated on a hot plate at 90 °C until a small (~10 μL) droplet of fuming concentrated sulfuric acid was obtained. This step ensured that Zr and Hf polymers were destroyed before processing the samples for Hf–Zr–REE separation. Although the formation of such polymers was not shown to disturb REE behavior in the column, they significantly modify Hf and Zr elution and may affect the overall efficiency of the separation (Strelow and Bothma, 1967). H_2SO_4 normality lower than 1 N should be avoided as an elution reagent because of the risk of repolymerization of Zr on the column (Strelow and Bothma, 1967). Hence, both fractions were introduced onto the resins in 1 N H_2SO_4 , which was obtained by diluting the H_2SO_4 droplets in 40 μL distilled water.

Two 200 μL cationic columns were prepared for REE separation from the spiked and unspiked aliquots. The samples were introduced in 50 μL of 1 N H_2SO_4 and Hf and Zr were eluted using 200 μL 1 N H_2SO_4 . Further purification was ensured by introducing 0.6 mL of 0.1 N HF onto the columns and the REE were subsequently recovered in 1 mL 4 N HCl. Purification of Nd from Ce and other REE was achieved by three successive passes onto a conventional HDEHP column (Eichrom™ Ln Spec). This separation method was preferred over the liquid–liquid extraction technique previously applied to whole-rock samples (Rehkamper et al., 1996; Caro et al., 2006) as the latter resulted in significant losses of material when small (ca. 10 ng) Nd samples were processed. Spiked Nd and Sm fractions were recovered in 0.24 N and 0.35 N HCl respectively after a single pass onto a 200 μL HDEHP column. Blanks and chemistry yields were identical to the garnet chemistry.

U–Pb analyses of zircons were carried out on a fraction of the dissolved sample aliquoted prior to REE separation. Chemical extraction of U and Pb was performed using 50 μL anion exchange columns. Blanks for the entire procedure were <1 pg Pb and 0.5 pg U. A mixed $^{205}\text{Pb}/^{235}\text{U}$ tracer solution was used for all analyses. Both Pb and U were loaded with 1 μL of silica gel-phosphoric acid mixture on outgassed single Re-filaments and measured on a MAT Finnigan 262 thermal ionisation mass spectrometer (ETH Zurich) using an ion counter system. The performance of the ion counter was checked by repeated measurements of the NBS 982 standard solution. The reproducibility of the $^{207}\text{Pb}/^{206}\text{Pb}$ ratio (0.467070) was better than 0.05 % (2σ). Hf isotope ratios in zircons were measured on a Nu Instruments multiple collector inductively coupled plasma mass spectrometer (ETH Zurich). Repeated measurements of JMC 475 standard yielded 0.282165 ± 10 (2σ) using the $^{179}\text{Hf}/^{177}\text{Hf} = 0.7325$ ratio for normalization (exponential law for mass correction). For the calculation of the ϵ_{Hf} values the following present-day ratios ($^{176}\text{Hf}/^{177}\text{Hf}$)_{CHUR} = 0.282772 and ($^{176}\text{Lu}/^{177}\text{Hf}$)_{CHUR} = 0.0332 were used (Blichert-Toft and Albarede, 1997), and an average $^{176}\text{Lu}/^{177}\text{Hf}$ ratio of 0.001 for all zircons was assumed in correcting the measured $^{176}\text{Hf}/^{177}\text{Hf}$ for radiogenic ingrowth (Harrison et al., 2005).

2.2. Mass spectrometry

Considering the small amount of material available for analysis, a series of tests was undertaken at low beam intensity in order to evaluate the internal and external precision of $^{142}\text{Nd}/^{144}\text{Nd}$ measurements and the limiting factors on both. Nd isotopes were measured using a

static collection mode with ^{144}Nd in the central cup. A double Re filament assembly was used and the samples were slowly heated (<30 mA/min) in order to obtain a stable ion beam. Internal precision is defined as $2\sigma_m = 2\sigma/\sqrt{n}$, where n is the number of individual ratios and σ is the standard deviation of the n ratios. External precision is defined as $2\sigma_e$, where σ_e is the standard deviation for a set of repeated analyses of the same sample. Note that the Ames solution used in this study (hereafter named IPGP Ames standard) was calibrated in 2001 against the LaJolla Nd standard using previously described analytical procedures (Caro et al., 2003). The results of this intercalibration (Table 1) show that a value of 0.511978 for the IPGP Ames solution corresponds to the reference value of 0.511860 for the LaJolla standard. Repeated analyses of this standard solution showed that the internal precision of $^{142}\text{Nd}/^{144}\text{Nd}$ measurements varies between 10 ppm and 40 ppm ($2\sigma_m$) when the ^{142}Nd ion beam intensity decreases from 5×10^{-11} A to 1×10^{-12} A (counting time ~ 100 min.), in close agreement with the uncertainty predicted by ion counting statistics using the Poisson law (Fig. 1A). Repeated measurements of Nd standard IPGP Ames

(Figs. 1B and 2) show that reproducibility of the $^{142}\text{Nd}/^{144}\text{Nd}$ analyses is approx. equal to the accuracy of individual measurements for Nd loads ranging from 10 ng ($2\sigma_e = 17$ ppm) to 500 ng ($2\sigma_e = 2$ ppm). This is remarkable given the many external sources of uncertainties (gain calibration, ion cup efficiencies, optical effects, etc.) which could potentially affect the reproducibility of the measurements. In contrast, the results shown in Fig. 1B indicate that the resolution of our measurements is limited solely by the mass of sample available and the ionization yield of Nd.

High (>5%) ionization yield can be obtained by analyzing neodymium as NdO^+ rather than Nd^+ . However, we chose to measure Nd as the metal ion in order to avoid the necessity of off-line corrections for $^{141}\text{Pr}^{17}\text{O}$ and $^{140}\text{Ce}^{18}\text{O}$ on $^{142}\text{Nd}^{16}\text{O}$, and eliminate uncertainties related to the isotopic composition of oxygen in the thermal-ionization source (Sharma et al., 1996). The ion yield obtained for measurements of 10–20 ng Nd as Nd^+ for the standard solution was $\sim 3\%$ and was generally higher than the yield obtained for larger loads ($\sim 2\%$). The corresponding internal precision was typically 15 ppm (2σ) for 10–20 ng loads (Fig. 2) and

Table 1
Inter-calibration results between LaJolla and IPGP Ames Nd standards

Run N. ^a	$^{142}\text{Nd}/^{144}\text{Nd}$	$^{143}\text{Nd}/^{144}\text{Nd}$	$^{145}\text{Nd}/^{144}\text{Nd}$	$^{148}\text{Nd}/^{144}\text{Nd}$	$^{150}\text{Nd}/^{144}\text{Nd}$	$^{146}\text{Nd}/^{144}\text{Nd}$ (measured)
LaJolla Cal.1	1.141802	0.511839	0.348401	0.241572	0.236433	0.721331
LaJolla Cal.2	1.141808	0.511838	0.348402	0.241576	0.236440	0.721176
LaJolla Cal.3	1.141808	0.511840	0.348403	0.241572	0.236437	0.722099
LaJolla Cal.4	1.141799	0.511846	0.348404	0.241575	0.236443	0.721531
LaJolla Cal.5	1.141797	0.511841	0.348403	0.241575	0.236434	0.721926
LaJolla Cal.6	1.141803	0.511842	0.348403	0.241574	0.236437	0.721571
LaJolla Cal.7	1.141798	0.511840	0.348402	0.241574	0.236434	0.721694
LaJolla Cal.8	1.141818	0.511842	0.348402	0.241576	0.236437	0.722054
LaJolla Cal.9	1.141804	0.511839	0.348403	0.241574	0.236436	0.721471
LaJolla Cal.10	1.141818	0.511843	0.348398	0.241577	0.236444	0.721337
LaJolla Cal.11	1.141810	0.511833	0.348400	0.241576	0.236438	0.721933
NdAmes Cal.1	1.141800	0.511955	0.348400	0.24157	0.236415	0.722862
NdAmes Cal.2	1.141806	0.511955	0.348400	0.241571	0.236421	0.721865
NdAmes Cal.3	1.141806	0.511954	0.348401	0.241572	0.236422	0.721878
NdAmes Cal.4	1.141804	0.511956	0.348399	0.241571	0.236420	0.721662
NdAmes Cal.5	1.141803	0.511954	0.348400	0.241572	0.236417	0.721775
NdAmes Cal.6	1.141803	0.511955	0.348402	0.241569	0.236417	0.723516
NdAmes Cal.7	1.141808	0.511957	0.348400	0.241571	0.236422	0.720406
NdAmes Cal.8	1.141814	0.511960	0.348402	0.241572	0.236424	0.721343
NdAmes Cal.9	1.141798	0.511956	0.348402	0.241567	0.236415	0.723229
NdAmes Cal.10	1.141804	0.511961	0.348404	0.241571	0.236419	0.722720
NdAmes Cal.11	1.141795	0.511960	0.348403	0.241568	0.236408	0.723048
NdAmes Cal.12	1.141803	0.511962	0.348405	0.241568	0.236415	0.723321
NdAmes Cal.13	1.141794	0.511961	0.348405	0.241567	0.236410	0.723184
Average IPGP Ames ^b	1.141806 (15)	0.511840 (6)	0.348402 (4)	0.241575 (4)	0.236437 (8)	
Average LaJolla ^b	1.141803 (11)	0.511958 (6)	0.348402 (4)	0.241570 (4)	0.236417 (9)	

^a Internal precisions for individual runs ($2\sigma_m$) were typically 8–10 ppm for $^{142}\text{Nd}/^{144}\text{Nd}$, 5 ppm for $^{143}\text{Nd}/^{144}\text{Nd}$, 5 ppm for $^{145}\text{Nd}/^{144}\text{Nd}$, 13–20 ppm for $^{148}\text{Nd}/^{144}\text{Nd}$ and 20–40 ppm for $^{150}\text{Nd}/^{144}\text{Nd}$. ^b Number in parenthesis represent the external reproducibility (2σ) for the repeated analyses of IPGP Ames and LaJolla standards.

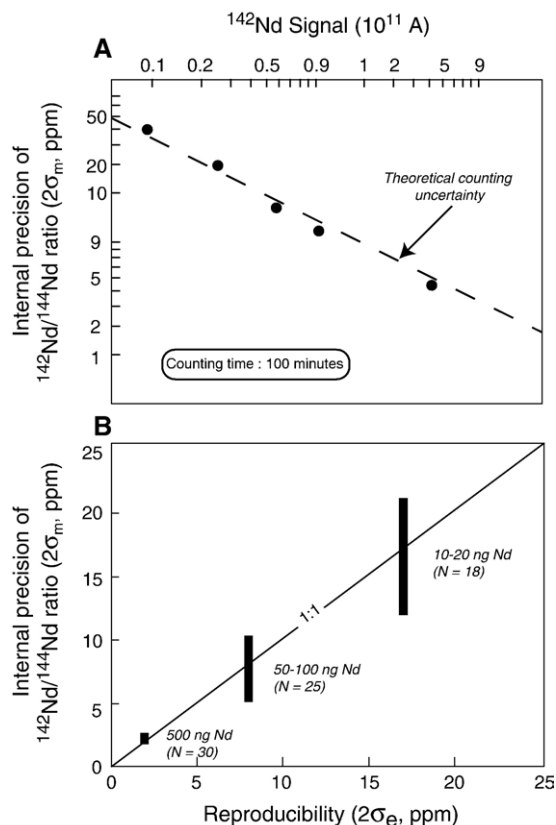


Fig. 1. A. Internal precision ($2\sigma_m$) of $^{142}\text{Nd}/^{144}\text{Nd}$ measurements as a function of ^{142}Nd intensity, compared with uncertainty predicted by ion counting statistics. Counting time was 100 minutes for all measurements. $^{142}\text{Nd}/^{144}\text{Nd}$ ratio was corrected from mass fractionation using the exponential law with $^{146}\text{Nd}/^{144}\text{Nd}=0.7219$ as normalization ratio. Theoretical uncertainty was calculated by propagating the counting errors ($1/\sqrt{I}$, where I is the total number of ions) for ^{142}Nd , ^{144}Nd and ^{146}Nd on the $^{142}\text{Nd}/^{144}\text{Nd}$ ratio. The decrease in internal precision with decreasing signal is entirely accounted for by the counting error as described by the Poisson Law. Consequently, the precision of Nd isotope ratios is not significantly affected by the noise of electronic components or any other source of scatter over the range of ion current investigated. B. Reproducibility and internal precision obtained for three different sets of $^{142}\text{Nd}/^{144}\text{Nd}$ measurements. Results for 500 ng Nd loads ($2\sigma_e=2$ ppm) are from Caro et al. (2006). $^{142}\text{Nd}/^{144}\text{Nd}$ data obtained for small (10–20 ng) Nd loads are plotted in Fig. 2. Results for these different datasets indicates that reproducibility of $^{142}\text{Nd}/^{144}\text{Nd}$ measurements is limited by counting statistics with no or negligible external source of error. Note that ^{142}Nd data showed here do not correspond to the inter-calibration measurements of the IPGP Ames standards presented in Table 1.

8 ppm (2σ) for 50–100 ng loads. Repeated analyses of an internal IPGP zircon standard yielded $^{142}\text{Nd}/^{144}\text{Nd}$ ratio indistinguishable from the IPGP Ames standard (Table 2). This indicates that no isobaric interference or matrix effects affected the accuracy of zircon measurements. We therefore consider that these techniques allow confident resolution of >25–30 ppm ^{142}Nd

anomalies in the Finsch sample and >15–20 ppm anomalies in the Jack Hills sample.

The main fraction of the Finsch composite yielded 15 ng Nd which was analyzed in a single run using a Finnigan Triton mass spectrometer (Institut de Physique du Globe de Paris). The samples were loaded and analyzed as described in Caro et al. (2006) but a static multicollection mode was preferred to a multi-dynamic scheme in order to maximize the counting time. The ^{142}Nd signal was maintained at a steady intensity of $0.5\text{--}1 \times 10^{-11}$ A during approx 90 minutes (ionization yield $\sim 3\%$), resulting in an uncertainty of 12 ppm ($2\sigma_m$) for the $^{142}\text{Nd}/^{144}\text{Nd}$ ratio. Both $^{142}\text{Ce}/^{142}\text{Nd}$ and $^{144}\text{Sm}/^{144}\text{Nd}$ ratios were monitored and found to be negligible (<1 ppm).

The main Jack Hills fraction yielded 70 ng Nd which was loaded and analyzed as described above. The main fraction yielded a long-lived (3 hr), intense ($^{142}\text{Nd}^+=10^{-11}$ A) beam, which allowed the determination of $^{142}\text{Nd}/^{144}\text{Nd}$ ratio with an internal precision of ± 10 ppm ($2\sigma_m$). Ion yield for this analysis was estimated to be $\sim 1.2\%$. ^{140}Ce and ^{147}Sm were monitored on Faraday cups and yielded $^{142}\text{Ce}/^{142}\text{Nd} \sim 10$ ppm and $^{144}\text{Sm}/^{144}\text{Nd} < 1$ ppm, respectively. A small correction was applied for the ^{142}Ce interference using $^{140}\text{Ce}/^{142}\text{Ce}=7.992$, while no correction was applied for $^{144}\text{Sm}/^{144}\text{Nd}$ interference.

3. Diamond inclusions from Finsch

^{147}Sm – ^{143}Nd investigations of inclusions in diamond have focused on establishing constraints on the age of crystallization of the host diamonds (e.g., Richardson et al., 1984, 1990, 1993). No ^{142}Nd investigation in diamonds and their inclusions has yet been conducted but a recent report suggests the presence

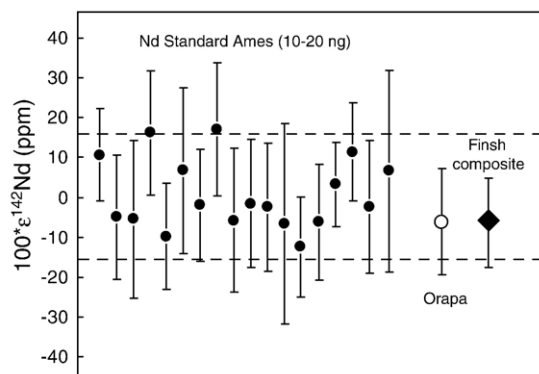


Fig. 2. ^{142}Nd result for the Finsch pyrope composite, compared with analyses of a garnet inclusion from Orapa (Botswana) and Nd standard IPGP Ames (10–20 ng loads). Reproducibility of standard measurements is 17 ppm ($2\sigma_e$).

Table 2
 $^{142,143}\text{Nd}$ results for Finsch pyropes and Jack Hills zircons

	Sm (ppm)	Nd (ppm)	$^{147}\text{Sm}/^{144}\text{Nd}$	Nd mass analyzed	$^{142}\text{Nd}/^{144}\text{Nd}$	100 ^a $\epsilon^{142}\text{Nd}$ (ppm)*	\pm	$^{143}\text{Nd}/^{144}\text{Nd}$	$\epsilon^{143}\text{Nd}^a$	\pm
<i>Samples</i>										
Finsch ^b	1.2	6.3	0.1150	15 ng	1.141816	-6	12	0.510974	-32.5	0.02
Jack Hills ^b	9.2	8.9	0.5891	65 ng	1.141832	8.2	10	0.514965	45.4	0.01
<i>Standards</i>										
Orapa Gt (N=1) ^b	0.5	0.9	0.3479	4 ng	1.141831	7	25	0.512775	2.7	0.03
Zircon Std (N=3) ^c	-	-	-	20 ng	1.141830	6	8	0.511985	-12.3	0.02
Ames Std (N=18) ^c	-	-	-	10–20 ng	1.141823	-	17	0.511953	-13.4	0.02

^a $\epsilon^{142}\text{Nd}$ is calculated using Ames standard average (1.141823) as reference value. $\epsilon^{143}\text{Nd}$ is calculated using $^{143}\text{Nd}/^{144}\text{Nd}=0.512638$ for the Chondritic Uniform Reservoir.

^b Uncertainties for Finsch, Jack Hills and Orapa are given as $2\sigma_m$.

^c A value of 0.511978 ± 10 ($n=11$) corresponds to a value for the LaJolla standard of 0.511860. The uncertainties for repeated Ames and Zircon standards measurements are given as $2\sigma_c$.

of a ~30 ppm excess in a lherzolitic nodule from Kimberley (Jagoutz and Dreibus, 2003). Such a result could reflect a link between the chemical characteristics of South African peridotites (Herzberg, 1993; Herzberg and Gasparik, 1991) and majorite segregation in a terrestrial magma ocean (Herzberg et al., 1988). Inclusions contained in diamonds should be more impervious to metasomatism than the peridotite themselves. Therefore, the study of Finsch pyrope inclusions was primarily undertaken in order to further investigate the ^{142}Nd signature of the lithospheric mantle beneath South Africa.

Analyzed samples are sub-calcic Cr-pyropes encapsulated in diamonds that were brought to the surface as xenoliths in a kimberlite 90 Ma ago (e.g. Boyd and Gurney, 1986). The peridotitic inclusions from Finsch are characterized by an equilibration temperature of 900–1100 °C for a pressure of 50 kb (Boyd and Finnerty, 1980). Lherzolitic nodules studied by Jagoutz and Dreibus (2003), on the other hand, belong to the low-temperature suite of South African peridotites. They are characterized by an equilibration temperature of 800 to 1000 °C and thus originate from shallower region of the Kaapvaal lithosphere (<150 km depth). The samples analyzed by Jagoutz and Dreibus (2003) are from the Kimberley mine, which is located only 160 km East of Finsch. The lherzolite samples studied by these authors and the diamond inclusions from this study thus originate from closely related regions of the South African lithosphere.

^{147}Sm – ^{143}Nd for Finsch are given in Table 2 and plotted in Fig. 3. ^{143}Nd results compare well with previous analyses from Richardson et al. (1984), confirming the mid-Archean age of diamond crystallization. The $\epsilon^{142}\text{Nd}$ of the inclusions is undistinguish-

able from the IGP Ames standard and modern terrestrial rock value (Table 2 and Fig. 2), yielding $100\times^{142}\text{Nd}=-6\pm 12$ ppm. In the absence of any obvious disturbance of the ^{147}Sm – ^{143}Nd system, modification of the $^{142}\text{Nd}/^{144}\text{Nd}$ ratio after diamond crystallization appears unlikely and we regard the measured ^{142}Nd signature in the pyrope garnets as that of their lithospheric source at the time of diamond crystallization.

Herzberg et al. (1988) noted that South African peridotites exhibit particular chemical properties (notably Al-depletion) and suggested that these could reflect majorite separation at high pressure in a global magma ocean. This proposition was echoed by Jagoutz and

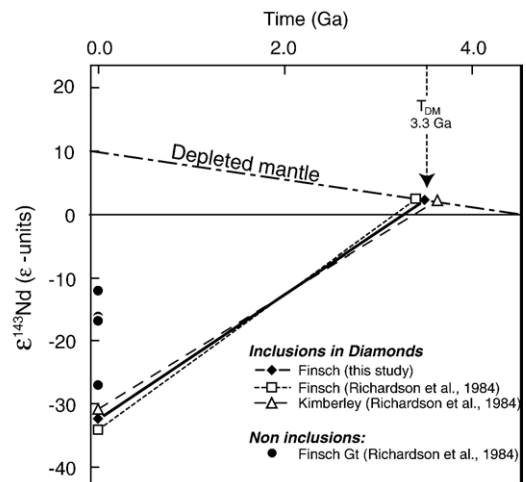


Fig. 3. $\epsilon^{143}\text{Nd}$ versus time plot illustrating the closed-system evolution of Pyrope inclusions from Finsch (This study and Richardson et al., 1984) and Kimberley (Richardson et al., 1984). All data are consistent with a mid-Archean (3.2–3.4 Ga) crystallization age for the diamonds. Garnet aggregates from Finsch kimberlite (Richardson et al., 1984) are also shown for comparison.

Dreibus (2003), who emphasized the chemical similarities between Kaapvaal peridotites and some martian meteorites, thought to record magma ocean processes. ^{142}Nd data do not provide direct constraints on majorite fractionation because Sm and Nd partition coefficients are so low in this mineral that unrealistically large amounts of majorite separation (>50%) would be needed to fractionate the Sm/Nd ratio in the residual liquid (see Fig. 5 of Corgne and Wood, 2004) to achieve a detectable ^{142}Nd anomaly. Indeed, Sm/Nd fractionation in a magma ocean is more likely controlled by the segregation of residual liquid from the solidifying mush but remains relatively unaffected by crystallization of major liquidus phases (Caro et al., 2005). Nevertheless, both mechanisms are expected to occur at different stages during the course of the crystallization of a magma ocean (Solomatov and Stevenson, 1993), and hence the chemical fractionation generated by majorite fractionation (i.e., Al depletion) and melt segregation (i.e., LREE depletion) should be superimposed in the uppermost mantle. The presence of positive ^{142}Nd anomalies in Archean rocks from West Greenland (Caro et al., 2003, 2006; Boyet and Carlson, 2006) were shown to indicate that such a process may have occurred early on in Earth history (Caro et al., 2005). The lack of ^{142}Nd anomaly in the Finsch sample suggests that the diamond inclusions have not preserved a record of Sm/Nd fractionation due to magma ocean crystallization. Although the potential role of metasomatism in eradicating ^{142}Nd heterogeneities in lithospheric mantle must always be considered (Richardson et al., 1984; Shimizu and Richardson, 1987), our results suggests that the South African lithosphere was likely formed at a time when ^{146}Sm decay had become negligible (i.e. > 4.2 Ga ago). Alternatively, the lack of a ^{142}Nd anomaly in these inclusions may indicate that convection remixed ^{142}Nd heterogeneities on a very fine scale prior to isolation of the South African lithosphere.

4. Jack Hills zircons

Nd isotope investigations in zircons have been mostly dedicated to geochronological studies of granitoids using the long-lived ^{147}Sm – ^{143}Nd system. (e.g Futa, 1986; Paterson et al., 1992; von Blanckenburg, 1992; von Quadt, 1992; Li, 1994; Poitrasson et al., 1998). Application of Sm–Nd systematics as a tracer of mantle–crust evolution was attempted by Amelin (2004) in a coupled U–Pb and ^{147}Sm – ^{143}Nd study of individual grains from Jack Hills. Unfortunately, the ^{147}Sm – ^{143}Nd system was shown to be variably disturbed and the precision of the data insufficient for

accurate correction of the $^{143}\text{Nd}/^{144}\text{Nd}$ ratio for in situ decay in the best-preserved grains. Amelin (2004) also reported ^{142}Nd data but the precision of the measurements was limited to 100 ppm due to the low Nd content of individual grains (<1 ng).

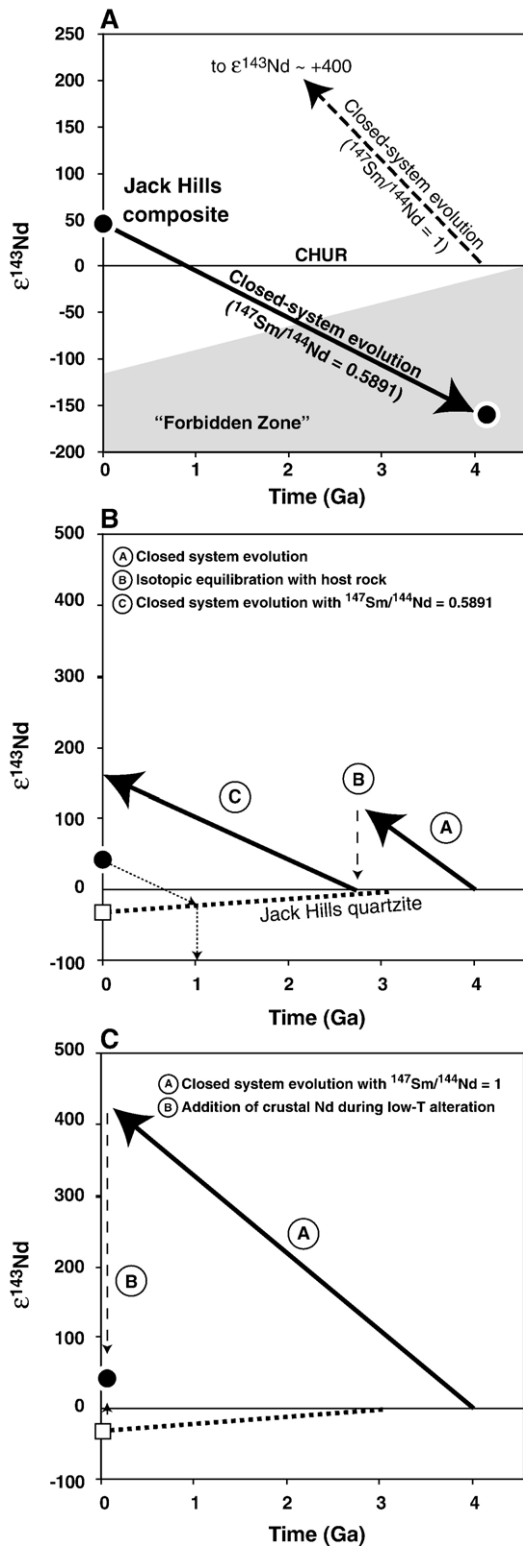
4.1. ^{176}Lu – ^{176}Hf , ^{146}Sm – ^{142}Nd and ^{147}Sm – ^{143}Nd systematics

^{176}Lu – ^{176}Hf results for the Jack Hills composite (Table 3) show good agreement with previous single grain analyses (Amelin et al., 1999; Harrison et al., 2005). Two replicates of the “Hf–Pb” aliquot yield a sub-chondritic initial $\epsilon_{\text{Hf}} \sim -6$ (using the parameters of Blichert-Toft and Albarède (1997) and Soderlund et al. (2004), and assuming an average zircon $^{176}\text{Lu}/^{177}\text{Hf}$ of 0.001; Harrison et al., 2005) indicating that grains analyzed in this study were derived from a reservoir characterized by long-term enrichment in incompatible elements. Assuming that this reservoir is continental crust with Lu/Hf~0.01 results in a CHUR model age of ~4.3 Ga. This model age should however be considered as a minimum given that: i) the crustal precursor may have been more mafic than average upper crust, and ii) the initial protolith may include components extracted from depleted mantle with positive ϵ_{Hf} (Harrison et al., 2005), and iii) younger, high-U zircon rims may contribute to underestimating the average age associated with calculation of ϵ_{Hf} . However, the Hf isotope results clearly indicate an ancient crustal signature for the Jack Hills composite. It is therefore expected that zircons formed from a protolith with sub-chondritic Sm/Nd ratio would exhibit negative initial $\epsilon^{143}\text{Nd}$ and $\epsilon^{142}\text{Nd}$.

^{147}Sm – ^{143}Nd results for the Jack Hills composite are given in Table 2 and plotted in Fig. 4A. Nd and Sm concentrations are fairly representative of previous single-grain analyses (e.g., Amelin, 2004; Maas et al., 1992) but suggest a LREE pattern with a slightly shallower slope than typical magmatic zircons ($^{147}\text{Sm}/^{144}\text{Nd} \sim 1$) (Hinton and Upton, 1991; Hoskin and Ireland, 2000; Hoskin, 2005). As can be seen from Fig. 4A, back-calculation of the present-day $^{143}\text{Nd}/^{144}\text{Nd}$ ratio yields an unrealistic estimate for the initial $\epsilon^{143}\text{Nd}$ of –160 which unambiguously indicates post-magmatic disturbance of the

Table 3
 ^{176}Lu – ^{176}Hf systematics of Jack Hills composite

	$^{176}\text{Hf}/^{177}\text{Hf}$	$\pm (2\sigma)$	$^{176}\text{Lu}/^{177}\text{Hf}$	ϵ_{Hf} (present)	ϵ_{Hf} (4.0 Ga)
JH-1	0.280103	0.000006	0.001	–94.39	–6.14
JH-2	0.280114	0.000007	0.001	–94.00	–5.75



^{147}Sm – ^{143}Nd system. Consequently, ^{147}Sm – ^{143}Nd systematics cannot provide any information on the age and composition of the parent crustal reservoir of Jack Hills zircons.

The main fraction of the Jack Hills composite yielded $100 \times ^{142}\text{Nd} = 8 \pm 10$ ppm ($2\sigma_m$), indistinguishable within errors from the Nd IPGP Ames standard (Table 2). This lack of a measurable ^{142}Nd anomaly is also consistent with open-system evolution as in-situ decay of ^{146}Sm in 4.0–4.1 Ga zircons with $^{147}\text{Sm}/^{144}\text{Nd} = 0.5891$ should generate a small (12–25 ppm) excess in $^{142}\text{Nd}/^{144}\text{Nd}$ over the IPGP Ames standard value. If a $^{147}\text{Sm}/^{144}\text{Nd}$ ratio of ~ 1 is assumed as the average Sm/Nd of Jack Hills zircons prior to disturbance, then an even larger anomaly (26–50 ppm) would be expected. The most likely explanation is that the ^{142}Nd excess initially developed in Jack Hills zircons has been overprinted by normal neodymium during a younger alteration event.

Another possibility is that zircons initially crystallized from a melt with negative $\epsilon^{142}\text{Nd}$ and subsequently evolved to their present-day value by *in situ* decay. Assuming, for example, that the crustal precursor was continental crust with $^{147}\text{Sm}/^{144}\text{Nd}$ ratio of ~ 0.1 , then 300 Ma would be needed for this reservoir to evolve from $100 \times ^{142}\text{Nd} = 0$ to $100 \times ^{142}\text{Nd}_{4\text{ Ga}} = -20$ ppm. This would require that the crustal reservoir from which the zircons ultimately formed was extracted from the mantle ~ 4.3 Ga ago, which would be consistent with the Hf isotope systematics. However, the manifest disturbance of the ^{147}Sm – ^{143}Nd system clearly indicates open system behavior of the grains with respect to LREE. In the next

Fig. 4. A. $\epsilon^{143}\text{Nd}$ versus time plot showing the closed system isotopic evolution of Jack Hills zircons since crystallization 4.1 Ga ago. The “forbidden zone” corresponds to isotopic compositions of reservoirs with negative Sm/Nd ratios. Back-calculation of the Jack Hills data at 4.0 Ga yields an initial $\epsilon^{143}\text{Nd}$ of -160 ϵ -units, which is obviously too low to represent a realistic estimate of the parent magma from which zircons crystallized. This clearly indicates that the Nd budget of the composite sample is partially controlled by grains having behaved as open-systems for ^{147}Sm – ^{143}Nd . The closed-system evolution of 4.0 Ga zircon with $^{147}\text{Sm}/^{144}\text{Nd} \sim 1$ is shown for comparison. B. Isotopic evolution of Jack Hills zircons assuming closed-system evolution since metamorphism of the Jack Hills quartzite 2.7 Ga ago. This scenario generates $^{143}\text{Nd}/^{144}\text{Nd}$ ratios largely more radiogenic than observed. A simple two-stage model (dashed arrow) shows that disturbance of the Sm–Nd systems must have occurred less than 1 Ga ago to account for the low measured $^{143}\text{Nd}/^{144}\text{Nd}$ ratio and thus postdates the major metamorphic events in the Jack Hills region (e.g. Cawood and Tyler, 2004). C. Expected effect of recent admixing of crustal Nd on the ^{147}Sm – ^{143}Nd systematics of Jack Hills zircons. Magmatic zircons first evolve as a closed system with $^{147}\text{Sm}/^{144}\text{Nd}$ ratios of ca. 1. Low-T alteration results in addition of non-radiogenic Nd from the surrounding host rock. This process is accompanied by a decrease in $^{147}\text{Sm}/^{144}\text{Nd}$ and $^{143}\text{Nd}/^{144}\text{Nd}$ ratios in altered grains.

Table 4
U–Pb results of Jack Hills composite

	U		Apparent ages (Ma)						Rho				
	(ppm)	Pb (ppm)	$^{206}\text{Pb}/^{204}\text{Pb}$	$^{206}\text{Pb}/^{238}\text{U}$	2 σ err. (%)	$^{207}\text{Pb}/^{235}\text{U}$	2 σ err. (%)	$^{207}\text{Pb}/^{206}\text{Pb}$		2 σ err. (%)	$^{206}\text{Pb}/^{238}\text{U}$	$^{207}\text{Pb}/^{235}\text{U}$	$^{207}\text{Pb}/^{206}\text{Pb}$
JH-1	165.7	104.3	5594.2	0.419577	0.48	24.5766	0.48	0.424824	0.0511	2258.6	3291.1	3999.4	0.99
JH-2	168.8	96.01	5112.5	0.422650	0.46	24.7498	0.46	0.424708	0.05	2272.5	3298.4	3998.9	0.99

section, we will examine alternative interpretations based on coupled examination of ^{146}Sm – ^{142}Nd and ^{147}Sm – ^{143}Nd systematics in the Jack Hills composite.

4.1.1. Possible causes of Sm–Nd disturbance

Several scenarios can potentially account for the disturbance of the ^{147}Sm – ^{143}Nd chronometer in Jack Hills zircons. These include i) isotopic equilibration and chronometer resetting during metamorphism, owing to enhanced REE exchange in radiation-damaged crystal lattices, ii) fluid-mediated recrystallization of metamict zircon rims accompanied by ion exchanges between fluids and recrystallized rims (Geisler et al., 2003a,b), or iii) crystallization or recrystallization of secondary rare earth minerals (e.g. monazite, xenotime) along fractures and/or partial replacement of zircon by hydrothermal minerals (e.g. zirconolite; Gieré, 1996). The first scenario can be ruled out immediately based on the observation that closed system evolution of the zircon since metamorphism of the Jack Hills 2.6–2.7 Ga ago (Kinny et al., 1988; Maas and McCulloch, 1991; Nutman et al., 1991; Trail et al., 2007b) would produce $^{143}\text{Nd}/^{144}\text{Nd}$ ratios markedly more radiogenic than that observed in the Jack Hills composite (Fig. 4B). As illustrated in Fig. 4B, the isotopic evolution of the zircons and that of the host sediment intersect at ca. 1 Ga, which we consider as an upper limit for the timing of disturbance. This age is not associated with any known tectono-metamorphic event in the Jack Hills region (Cawood and Tyler, 2004; Dunn et al., 2005) and is probably meaningless. However, this observation indicates that perturbation of the Sm–Nd system occurred recently and in relation with low-temperature alteration processes.

Further support for recent, low-T alteration of the Jack Hills zircons is provided by U–Pb isotope systematics. As shown in Table 4 and Fig. 5, analysis of the bulk sample confirms the old average $^{206}\text{Pb}/^{207}\text{Pb}$ age (~4.0 Ga) obtained by the SHRIMP method. However, the Pb isotopic composition of the composite sample is characterized by substantially greater U–Pb discordance than that detected by SHRIMP analyses (i.e., <10% discordance). These results show that a

significant fraction of the U–Pb system (i.e., potentially a small fraction of the sample mass) in the analyzed grains experienced Pb loss at a recent time. Similar discordia trending to present day are not uncommon within the Jack Hills population (Froude et al., 1983; Maas et al., 1992; Peck et al., 2001; Nemchin et al., 2006; Trail et al., 2007b). Our observations suggest that the recent episode of alteration which resulted in loss of radiogenic Pb was also probably associated with disturbance of Sm–Nd systematics and LREE enrichment (see Section 4.2.3). The discrepancy observed between bulk and in situ analyses suggests that altered material is primarily located within thin rims and is therefore under-represented in the analyses of polished cross sections by ion microprobe analysis (Trail et al., 2007b).

4.1.2. A mixing model for Nd isotopes in the Jack Hills composite

^{147}Sm – ^{143}Nd data for the Jack Hills composite are plotted in Fig. 6 together with single-grain analyses from Amelin (2004). The data define a pseudo-isochron with an apparent age of ca. 4 Ga. In such a diagram, however, a mixing relationship is a straight line, such that the observed correlation is best explained by recent admixing of material with low $^{147}\text{Sm}/^{144}\text{Nd}$ and

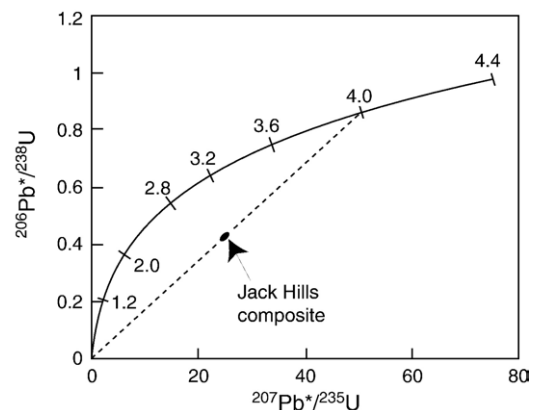


Fig. 5. U–Pb results for the Jack Hills composite. A discordia with lower intercept at $T=0$ and upper intercept at $T=4$ Ga is shown as a visual guide (dashed line).

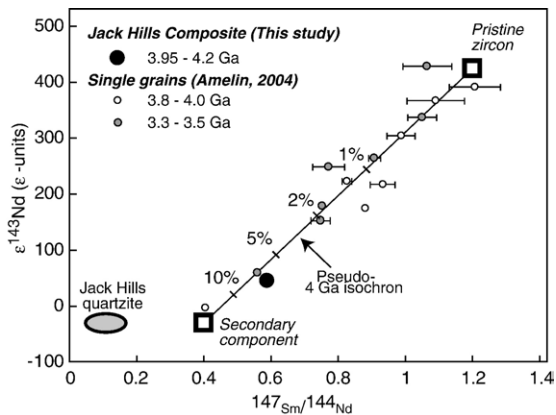


Fig. 6. $^{147}\text{Sm}/^{144}\text{Nd}$ systematics of Jack Hills composite compared with single grain analyses from Amelin (2004). A mixing relationship between LREE-poor, unaltered zircons ($^{147}\text{Sm}/^{144}\text{Nd}=1$, $^{143}\text{Nd}/^{144}\text{Nd}=0.534$, $[\text{Nd}]=1.5$ ppm) and LREE-rich altered material ($^{147}\text{Sm}/^{144}\text{Nd}=0.3$, $^{143}\text{Nd}/^{144}\text{Nd}=0.514$, $[\text{Nd}]=100$ ppm) is plotted for comparison. See text for discussion on parameters used in model calculation.

$^{143}\text{Nd}/^{144}\text{Nd}$ ratios with the highly radiogenic ~ 4 Ga old zircons (Amelin, 2004). Assuming that the secondary component is not less radiogenic than the host metasediment, then a $^{147}\text{Sm}/^{144}\text{Nd}$ ratio of ~ 0.4 can be estimated from the correlation of Fig. 6. This value is suggestive of a LREE-pattern with shallow slope, in contrast with the characteristic steep LREE pattern of magmatic zircons ($^{147}\text{Sm}/^{144}\text{Nd}\sim 1$).

Grains with flat LREE patterns and high Nd contents (50–200 ppm) have been reported from several studies of the Jack Hills zircons (e.g. Maas et al., 1992) and from West Greenland (e.g. Whitehouse and Kamber, 2002). Hoskin (2005) and Nemchin et al. (2006) proposed that the high LREE-patterns in Jack Hills were produced by post-magmatic alteration processes, during which cation and isotope exchanges occur between hydrothermal fluid and zircons during recrystallization of amorphized grains. Such processes were also documented by Pidgeon et al. (1966) and Geisler et al. (2003a,b) and were shown to be accompanied by severe Pb-loss. Cavosie et al. (2005) also reported local LREE-enrichment in Jack Hills grains, and found these to be associated with Si-depletion, P-enrichment, and U–Pb discordance. However, these authors found no correlated effect with oxygen isotopes, which led them to favor the presence of secondary subsurface minerals (e.g. monazite, xenotime) over models involving fluid-mediated recrystallization. Note that the presence of primary inclusions of apatite, monazite or xenotime could also produce LREE-enrichment in the grains. However, primary inclusions cannot account for the Sm–Nd systematics of the Jack Hills composite as these are

essentially contemporaneous of zircon formation (Trail et al., 2004). Their presence would thus not affect the Nd model age of the sample. The young model age of ~ 1 Ga obtained for the Jack Hills composite can only be explained by recent alteration of the LREE budget of the zircons.

^{147}Sm – ^{143}Nd systematics in zircons from Cavosie et al. (2005) clearly indicates that the LREE-rich regions observed by these authors contain non-radiogenic Nd recently added to the zircon and therefore represent a secondary product rather than a feature of the magma from which zircons crystallized. Regardless of the exact nature of this recent component (recrystallized rims and/or subsurface inclusions), the Nd isotope signature of

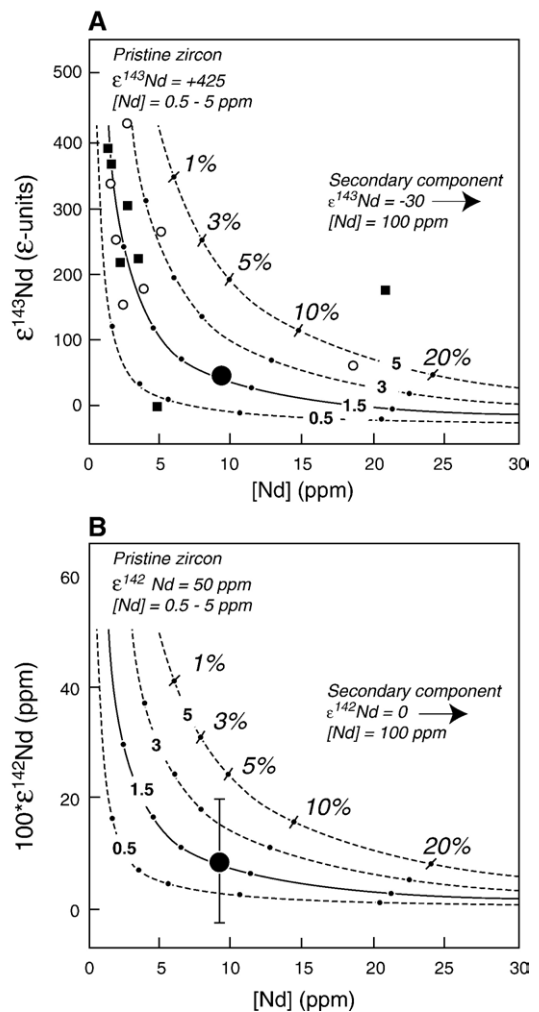


Fig. 7. Mixing hyperbolae showing the effect of LREE enrichment during low-T alteration on A. $^{143}\text{Nd}/^{144}\text{Nd}$ and B. $^{142}\text{Nd}/^{144}\text{Nd}$ ratios of Jack Hills zircons. LREE-rich secondary material may account for only 5% to 10% of the total mass of sample analyzed but contains $\sim 90\%$ of the Nd budget of the Jack Hills sample.

the Jack Hills sample should hence be accounted for by a simple mixing model with negligible radiogenic ingrowth since the time of disturbance (Fig. 4C). In order to test the consistency of this scenario with regards to ^{142}Nd and ^{143}Nd data, we calculated the isotopic composition of a binary mixture of pristine zircon with a secondary, unradiogenic component characterized by high Nd content. In this model, the secondary component is analogous to type 2 compositions from Hoskin (2005) and Cavosie et al. (2005). This secondary component is considered to contain crustal Nd with $\epsilon^{143}\text{Nd}$ identical to that of the present-day host rock (Maas, 1992) and an Nd content of ~ 100 ppm. The latter value is representative of the most LREE-rich compositions measured in Jack Hills grains (Maas and McCulloch, 1991; Cavosie et al., 2005; Hoskin, 2005). The pristine zircon end-member (equivalent to type 1 compositions from Hoskin (2005) and Cavosie et al. (2005)) is considered to have evolved since 4.0 Ga with a $^{147}\text{Sm}/^{144}\text{Nd}$ ratio of ca. 1 and Nd content of 0.5 to 5 ppm. Results of this calculation show that the ^{143}Nd signature of the Jack Hills composite can be matched by the proposed mixing relationship assuming that the secondary end-member composes 5 to 10% of the entire sample (Fig. 7A). This percentage is similar to the frequency of occurrence of type-2 patterns ($\sim 8\%$) in the survey of Jack Hills grains performed by Cavosie et al. (2005). Our model also provides a satisfactory explanation for the absence of ^{142}Nd anomaly as the 50 ppm excess developed by in-situ decay in pristine zircons is overprinted below detection limit by addition of only 3% of such secondary material (Fig. 7B).

Further examination of Sm–Nd systematics in Jack Hills zircons would clearly benefit from a better knowledge of the processes affecting rare earth elements during alteration of metamict grains. Indeed, our results indicate that the Nd isotope record in Jack Hills has only been partially overprinted and this record may hence be recovered if secondary components can be selectively removed from the zircons. If the budget of LREE is controlled by secondary minerals, then leaching zircon powders in acid prior to dissolution may permit removal of secondary Nd. Alternatively, a mild leaching of bulk zircons in HF may reduce the mass fraction of recrystallized rims compared with preserved grain interiors.

5. Conclusions

Our results demonstrate the feasibility of ^{142}Nd analyses at high precision (10–20 ppm) in samples containing as little as 10 ng Nd. Using these techniques,

we investigated ^{146}Sm – ^{142}Nd systematics in inclusions in diamonds from South Africa and a composite sample of Jack Hills zircons from Western Australia. The analyses of garnet inclusions do not confirm a previous report of a high $^{142}\text{Nd}/^{144}\text{Nd}$ in lithospheric mantle beneath the South African craton. The lack of a ^{142}Nd anomaly in these inclusions may be indicative that convection remixed ^{142}Nd heterogeneities on a very fine scale prior to isolation of the South African lithosphere. Alternatively, this result may indicate that a significant fraction of the mantle never developed detectable ^{142}Nd anomalies following early terrestrial differentiation. Analysis of ca. 4.0 Ga detrital zircons from Jack Hills shows that $^{142,143}\text{Nd}/^{144}\text{Nd}$ ratios were modified by post-depositional low temperature alteration. This disturbance resulted in a binary mixing between LREE-rich, unradiogenic material and radiogenic Nd from the pristine ~ 4 Ga zircons. This secondary component could be present either as secondary rims or as secondary REE-rich minerals located along fractures and/or pitted grain surfaces.

Acknowledgements

We thank Pierre Cartigny for support at the early stage of the study of diamonds, and Emilie Thomassot, who provided the garnet inclusions from Orapa. Urs Schärer is acknowledged for his assistance during the development of analytical procedures for zircon dissolution. We thank M. Sharma and an anonymous reviewer for their helpful comments and criticisms. This work was supported by grants from the IGP Graduate School (GC), ARC grant DP0666497 and NSF grant EAR-0635969 (TMH), the NASA Exobiology grant NAG5-13497 (SJM), and by facility support from the Instrumentation and Facilities Program of the National Science Foundation.

References

- Amelin, Y., 2004. Sm–Nd systematics of zircon. *Chem. Geol.* 211 (3–4), 375–387.
- Amelin, Y., Lee, D.C., Halliday, A.N., Pidgeon, R.T., 1999. Nature of the Earth's earliest crust from hafnium isotopes in single detrital zircons. *Nature* 399 (6733), 252–255.
- Blichert-Toft, J., Albarède, F., 1997. The Lu–Hf geochemistry of chondrites and the evolution of the mantle–crust system. *Earth Planet. Sci. Lett.* 148, 243–258.
- Boyd, F.R., Finnerty, A.A., 1980. Conditions of origin of natural diamonds of peridotites affinity. *J. Geophys. Res.* 85, 6911–6918.
- Boyd, F.R., Gurney, J.J., 1986. Diamonds and the African Lithosphere. *Science* 232, 254–258.
- Boyet, M., Carlson, R.W., 2006. A new geochemical model for the Earth's mantle inferred from ^{146}Sm – ^{142}Nd systematics. *Earth Planet. Sci. Lett.* 250, 254–258.

- Caro, G., Bourdon, B., Birck, J.-L., Moorbath, S., 2003. ^{146}Sm – ^{142}Nd evidence for early differentiation of the Earth's mantle. *Nature* 423, 428–432.
- Caro, G., Bourdon, B., Wood, B.J., Corgne, A., 2005. Trace element fractionation generated by melt segregation from a magma ocean. *Nature* 436, 246–249.
- Caro, G., Bourdon, B., Birck, J.-L., Moorbath, S., 2006. High-precision $^{142}\text{Nd}/^{144}\text{Nd}$ measurements in terrestrial rocks: Constraints on the early differentiation of the Earth's mantle. *Geochim. Cosmochim. Acta* 70, 164–191.
- Cavosie, A.J., Valley, J.W., Wilde, S.A., E.I.M.F., 2005. Magmatic $\delta^{18}\text{O}$ in 4400–3900 Ma detrital zircons: A record of the alteration and recycling of crust in the Early Archean. *Earth Planet. Sci. Lett.* 235, 663–681.
- Cawood, P.A., Tyler, I.M., 2004. Assembling and reactivating the Proterozoic Capricorn Orogen: lithotectonic elements, orogenies, and significance. *Precambrian Res.* 128, 201–218.
- Cherniak, D.J., Hanchar, J.M., Watson, E.B., 1997. Rare-earth diffusion in zircon. *Chem. Geol.* 134, 289–301.
- Corgne, A., Wood, B.J., 2004. Trace element partitioning between majoritic garnet and silicate melt at 25 GPa. *Phys. Earth Planet. Inter.* 143–144, 407–419.
- Dunn, S.J., Nemchin, A.A., Cawood, P.A., Pidgeon, R.T., 2005. Provenance record of the Jack Hills metasedimentary belt: Source of the Earth's oldest zircons. *Precambrian Res.* 138, 235–254.
- Froude, D.O., et al., 1983. Ion microprobe identification of 4100–4200 Myr old terrestrial zircons. *Nature* 304, 616–618.
- Futa, K., 1986. Sm–Nd isotope systematics of a tonalitic augen gneiss and its constituent minerals from northern Michigan. *Geochim. Cosmochim. Acta* 45, 1245–1249.
- Geisler, T., Pidgeon, R.T., Kurtz, R., Bronswijk, W.V., Schleicher, H., 2003a. Experimental hydrothermal alteration of partially metamict zircon. *Am. Mineral.* 88, 1496–1513.
- Geisler, T., et al., 2003b. Low-Temperature hydrothermal alteration of natural metamict zircons from the Eastern Desert, Egypt. *Mineral. Mag.* 67 (3), 485–508.
- Gieré, R., 1996. The formation of rare earth minerals in hydrothermal systems. In: Jones, A.P., Wall, F., Williams, C.T. (Eds.), *Rare Earth Minerals: Chemistry, Origin and Ore Deposits*. The Mineralogical Society Series.
- Goldstein, S.L., Galer, S.J.G., 1992. On the trail of early mantle differentiation: $^{142}\text{Nd}/^{144}\text{Nd}$ ratios of early Archean rocks. *Eos Trans. AGU* 73, S323.
- Hoskin, P.W.O., Schaltegger, U., 2003. The composition of zircon and igneous and metamorphic petrogenesis. In: Hanchar, J.M., Hoskin, P.W.O. (Eds.), *Zircon*. *Rev. Mineral. Geochem.*, 53. Mineralogical Society of America, Washington, D.C., pp. 27–62.
- Harper, C.L., Jacobsen, S.B., 1992. Evidence from coupled ^{147}Sm – ^{143}Nd and ^{146}Sm – ^{142}Nd systematics for very early (4.5 Gyr) differentiation of the Earth's mantle. *Nature* 360, 728–732.
- Harrison, T.M., et al., 2005. Heterogeneous Hadean hafnium: Evidence of continental crust at 4.4 to 4.5 Ga. *Science* 310, 1947–1950.
- Herzberg, C.T., 1993. Lithosphere peridotites of the Kaapvaal craton. *Earth Planet. Sci. Lett.* 120, 13–29.
- Herzberg, C.T., Gasparik, T., 1991. Garnet and pyroxenes in the mantle: a test of the majorite fractionation hypothesis. *J. Geophys. Res.* 96, 16,263–16,274.
- Herzberg, C.T., Feingerson, M., Cherylyn, S., Ohtani, E., 1988. Majorite fractionation recorded in the geochemistry of peridotites from South Africa. *Nature* 332, 823–826.
- Hinton, R.W., Upton, B.G.J., 1991. The chemistry of zircon — variations within and between large crystals from syenite and alkali basalt xenoliths. *Geochim. Cosmochim. Acta* 55, 3287–3302.
- Hoskin, P.W.O., 2005. Trace-element composition of hydrothermal zircon and the alteration of Hadean zircon from the Jack Hills, Australia. *Geochim. Cosmochim. Acta* 69, 637–648.
- Hoskin, P.W.O., Ireland, T.R., 2000. Rare earth element chemistry of zircon and its use as a provenance indicator. *Geology* 28, 627–630.
- Ireland, T.R., et al., in press. The coupled development of SHRIMP and analysis of Hadean zircons. *Austr. J. Earth Sci.*
- Jagoutz, E., Dreibus, G., 2003. On the search for ^{142}Nd in terrestrial rocks. 8th kimberlite conference abstract.
- Kinny, P.D., Wijbrans, J.R., Froude, D.O., Ireland, T.R., Compston, W., 1988. Age constraints on the geological evolution of the Narryer gneiss complex, Western Australia. *Aust. J. Earth Sci.* 37, 51–69.
- Li, X., 1994. A comprehensive U–Pb, Sm–Nd, Rb–Sr and ^{40}Ar – ^{39}Ar geochronological study of the Guidong granodiorite, southeast China: records of multiple tectono–thermal events in a single pluton. *Chem. Geol.* 115, 283–295.
- Maas, R., McCulloch, M.T., 1991. The provenance of Archean clastic metasediments in the Narryer Gneiss Complex, Western Australia: trace element geochemistry, Nd isotopes and U–Pb ages for detrital zircons. *Geochim. Cosmochim. Acta* 55, 1915–1932.
- Maas, R., Kinny, P.D., Williams, I.S., Froude, D.O., Compston, W., 1992. The Earth's oldest crust: a chronological and geochemical study of 3900–4200 Ma old detrital zircons from Mt. Narryer and Jack Hills, Western Australia. *Geochim. Cosmochim. Acta* 56, 1281–1300.
- McCulloch, M.T., Bennett, V.C., 1993. Evolution of the early Earth: Constraints from ^{143}Nd – ^{142}Nd isotopic systematics. *Lithos* 30, 237–255.
- Mojzsis, S.J., Harrison, T.M., Pidgeon, R.T., 2001. Oxygen-isotope evidence from ancient zircons for liquid water at the Earth's surface 4300 Myr ago. *Nature* 409, 178–181.
- Nemchin, A.A., Pidgeon, R.T., Whitehouse, M.J., 2006. Re-evaluation of the origin and evolution of >4.2 Ga zircons from the Jack Hills metasedimentary rocks. *Earth Planet. Sci. Lett.* 244, 218–233.
- Nutman, A.P., Kinny, P.D., Compston, W., Williams, I.S., 1991. SHRIMP U–Pb zircon geochronology of the Narryer Gneiss Complex, Western Australia. *Precambrian Res.* 52, 275–300.
- Paterson, B.A., Rogers, G., Stephens, W.E., 1992. Evidence for inherited Sm–Nd isotopes in granitoid zircons. *Contrib. Mineral. Petrol.* 111, 378–390.
- Peck, W.H., Valley, J.W., Wilde, S.A., Graham, C.M., 2001. Oxygen isotope ratios and rare earth elements in 3.3 to 4.4 Ga zircons: ion microprobe evidence for high $\delta^{18}\text{O}$ continental crust and oceans in the Early Archean. *Geochim. Cosmochim. Acta* 65, 4215–4229.
- Pidgeon, R.T., O'Neil, J.R., Silver, L.T., 1966. Uranium and Lead isotopic stability in a metamict zircon under experimental hydrothermal conditions. *Science* 154, 1538–1966.
- Poitrasson, F., Paquette, J.-L., Montel, J.-M., Pin, C., Duthou, J.-L., 1998. Importance of late-magmatic and hydrothermal fluids on the Sm–Nd isotope mineral systematics of hypersolvus granites. *Chem. Geol.* 146, 187–203.
- Rehkamper, M., Gartner, M., Galer, S.J.G., Goldstein, S.L., 1996. Separation of Ce from other rare-earth elements with application to Sm–Nd and La–Ce chronometry. *Chem. Geol.* 129 (3–4), 201–208.
- Richardson, S.H., Gurney, J.J., Erlank, A.J., Harris, J.W., 1984. Origin of diamonds in old enriched mantle. *Nature* 310, 198–202.
- Richardson, S.H., Erlank, A.J., Harris, J.W., Hart, S.R., 1990. Eclogitic diamonds of Proterozoic age from Cretaceous kimberlites. *Nature* 346, 54–56.
- Richardson, S.H., Harris, J.W., Gurney, J.J., 1993. Three generations of diamonds from old continental mantle. *Nature* 366, 256–258.

- Sharma, M., Papanastassiou, D.A., Wasserburg, G.J., Dymek, R.F., 1996. The issue of the terrestrial record of ^{146}Sm . *Geochim. Cosmochim. Acta* 60, 2037–2047.
- Shimizu, N., Richardson, S.H., 1987. Trace-element abundance patterns of garnet inclusions in peridotite-suite diamonds. *Geochim. Cosmochim. Acta* 51, 755–758.
- Solomatov, V.S., Stevenson, D.J., 1993. Non-fractional crystallization of a terrestrial magma ocean. *J. Geophys. Res.* 98 (E3), 5391–5406.
- Soderlund, U., Patchett, J.P., Vervoort, J.D., Isachsen, C.E., 2004. The Lu-176 decay constant determined by Lu–Hf and U–Pb systematics of Precambrian mafic intrusions. *Earth Planet. Sci. Lett.* 219, 311–324.
- Strelow, F.W.E., Bothma, C.J.C., 1967. Anion exchange and a selectivity scale for elements in sulfuric acid media with a strongly basic resin. *Anal. Chem.* 39, 595–599.
- Trail, D., Catlos, E.J., Harrison, T.M., Mojzsis, S.J., 2004. New analyses of diverse Hadean zircon inclusions from Jack Hills, Western Australia: XXXV Lunar and Planetary Science Conference, Houston, Texas.
- Trail, D., et al., 2007a. Constraints on Hadean zircon protoliths from oxygen isotopes, Ti-thermometry, and rare earth elements. *Geochim. Geophys. Geosyst.* 8, Q06014. doi:10.1029/2006GC001449.
- Trail, D., Mojzsis, S.J., Harrison, T.M., 2007b. Thermal events documented in Hadean zircons by ion microprobe depth profiles. *Geochim. Cosmochim. Acta* 71, 4044–4065.
- von Blanckenburg, F., 1992. Combined high-precision chronometry and geochemical tracing using accessory minerals: applied to Central-Alpine Bergell intrusion (central Europe). *Chem. Geol.* 100, 19–40.
- von Quadt, A., 1992. U–Pb and Sm–Nd geochronology of mafic and ultramafic rocks from the central part of the Tauern Window (eastern Alps). *Contrib. Mineral. Petrol.* 110, 57–67.
- Wilde, S.A., Valley, J.W., Peck, W.H., Graham, C.M., 2001. Evidence from detrital zircons for the existence of continental crust and oceans on the Earth 4.4 Gyr ago. *Nature* 409, 175–178.
- Whitehouse, M.J., Kamber, B.S., 2002. On the overabundance of light rare earth elements in terrestrial zircons and its implication for Earth's earliest magmatic differentiation. *Earth Planet. Sci. Lett.* 204, 333–346.